

# Properties of universal bosonic tetramers <sup>\*</sup>

A. Deltuva

Received: date / Accepted: date

**Abstract** The system of four identical bosons is studied using momentum-space equations for the four-particle transition operators. Positions, widths and existence limits of universal unstable tetramers are determined with high accuracy. Their effect on the atom-trimer and dimer-dimer scattering observables is discussed. We show that a universal shallow tetramer intersects the atom-trimer threshold twice leading to resonant effects in ultracold atom-trimer collisions.

**Keywords** Efimov effect · four-particle scattering

**PACS** 34.50.-s · 31.15.ac

## 1 Introduction

Few-particle systems with resonant interactions are universal in the sense that their properties are independent of the short-range interaction details. Well known example is the Efimov effect, where in the unitary limit, characterized by the two-particle scattering length  $a \rightarrow \infty$ , an infinite number of weakly bound trimers with zero spin and positive parity ( $0^+$ ) may exist [1]. Furthermore, Refs. [3, 4] predicted the existence of two  $0^+$  tetramers for each Efimov trimer. The two lowest tetramers, i.e., the ones associated with the trimer ground state, are true bound states and have already been studied extensively [3, 4, 10]; however, they may be affected significantly by the finite-range corrections such that even some contradictions between Refs. [3, 4] and [10] exist. In contrast, all other tetramers lie above the lowest particle-trimer threshold and therefore have finite width and lifetime. Thus, although a number of sophisticated numerical methods [3, 4, 10, 11] is available for the four-boson bound states, not all of them can be applied to a rigorous study of higher tetramers; a proper treatment of the continuum is needed. However, in this case the technical difficulties in describing the scattering processes involving

---

<sup>\*</sup> Special issue devoted to Critical Stability 2011

very weakly bound dimers and trimers in the universal regime may limit the accuracy of the coordinate-space methods [12, 13]. Alternative calculations using the momentum-space framework have been recently performed by us for the atom-trimer [8] and dimer-dimer [9] scattering. The description is based on the exact four-particle Alt, Grassberger, and Sandhas (AGS) equations [14] for the transition operators. The numerical technique, with some important modifications, is taken over from the four-nucleon scattering calculations [15, 16]. In this work it will be used to determine the universal properties of unstable tetramers. While their positions and limits of existence have already been calculated using coordinate-space methods [4, 17], in our momentum-space framework we are able to achieve the universal limit with much higher accuracy, revealing in some cases quite drastic differences as compared to the predictions of Refs. [4, 17]. Furthermore, we obtain results for the widths of the tetramers.

In Sec. 2 we describe the employed four-boson scattering equations and the technical framework. In Sec. 3 we present results for tetramer properties and their effect on the atom-trimer and dimer-dimer scattering observables; we also compare our predictions with those by other authors. We summarize in Sec. 4.

## 2 Four-boson scattering equations

An exact description of the four-particle scattering can be given by the Faddeev-Yakubovsky equations [18] for the wave-function components or by the equivalent Alt, Grassberger, and Sandhas (AGS) equations [14] for the transition operators; the latter are more convenient to solve in the momentum-space framework preferred by us. The number of independent transition operators (wave-function components) is significantly reduced in the case of four identical particles where there are only two distinct two-cluster partitions, one of  $3 + 1$  type and one of  $2 + 2$  type. We choose those partitions to be  $(12,3)4$  and  $(12)(34)$  and denote them in the following by  $\alpha = 1$  and  $2$ , respectively. The corresponding transition operators  $\mathcal{U}_{\beta\alpha}$  for the system of four identical bosons obey symmetrized AGS equations

$$\mathcal{U}_{11} = P_{34}(G_0 t G_0)^{-1} + P_{34} U_1 G_0 t G_0 \mathcal{U}_{11} + U_2 G_0 t G_0 \mathcal{U}_{21}, \quad (1a)$$

$$\mathcal{U}_{21} = (1 + P_{34})(G_0 t G_0)^{-1} + (1 + P_{34}) U_1 G_0 t G_0 \mathcal{U}_{11}, \quad (1b)$$

$$\mathcal{U}_{12} = (G_0 t G_0)^{-1} + P_{34} U_1 G_0 t G_0 \mathcal{U}_{12} + U_2 G_0 t G_0 \mathcal{U}_{22}, \quad (1c)$$

$$\mathcal{U}_{22} = (1 + P_{34}) U_1 G_0 t G_0 \mathcal{U}_{12}. \quad (1d)$$

Here  $G_0 = (E + i0 - H_0)^{-1}$  is the free Green's function of the four-particle system with energy  $E$  and kinetic energy operator  $H_0$ , the two-particle transition matrix  $t$  acting within the pair  $(12)$  is derived from the corresponding potential  $v$  using the Lippmann-Schwinger equation

$$t = v + v G_0 t, \quad (2)$$

and the symmetrized operators for the  $1+3$  and  $2+2$  subsystems are obtained from the integral equations

$$U_\alpha = P_\alpha G_0^{-1} + P_\alpha t G_0 U_\alpha. \quad (3)$$

The employed basis states have to be symmetric under exchange of two particles in subsystem  $(12)$  for  $3 + 1$  partition and in  $(12)$  and  $(34)$  for  $2 + 2$  partition.

The correct symmetry of the four-boson system is ensured by the operators  $P_{34}$ ,  $P_1 = P_{12} P_{23} + P_{13} P_{23}$ , and  $P_2 = P_{13} P_{24}$  where  $P_{ab}$  is the permutation operator of particles  $a$  and  $b$ .

All observables for two-cluster reactions are determined by the transition amplitudes

$$\langle \Phi_\beta^f | T | \Phi_\alpha^i \rangle = S_{\beta\alpha} \langle \phi_\beta^f | \mathcal{U}_{\beta\alpha} | \phi_\alpha^i \rangle, \quad (4)$$

obtained [19] as on-shell matrix elements of the AGS operators (1); the weight factors  $S_{\beta\alpha}$  with values  $S_{11} = 3$ ,  $S_{22} = 2$ , and  $S_{12} = 2S_{21} = 2\sqrt{3}$  arise due to the symmetrization [20]. The matrix elements (4) are calculated between the Faddeev components

$$|\phi_\alpha^n\rangle = G_0 t P_\alpha |\phi_\alpha^n\rangle \quad (5)$$

of the corresponding initial/final atom-trimer or dimer-dimer states  $|\Phi_\alpha^n\rangle = (1 + P_\alpha)|\phi_\alpha^n\rangle$ .

The calculation of scattering observables is done at real energies  $E = \varepsilon_\alpha^n + p_\alpha^n^2/2\mu_\alpha$  where  $-\varepsilon_\alpha^n$  is the binding energy of the initial  $n$ th state in the  $\alpha$  channel,  $p_\alpha^n$  is the corresponding relative two-cluster momentum, and  $\mu_\alpha$  the reduced two-cluster mass. However, in the spin/parity  $0^+$  states at complex energy values  $E = E_r = -B_r - i\Gamma_r/2$ , corresponding to each unstable tetramer with energy  $-B_r$  (relative to the four-body breakup threshold) and width  $\Gamma_r$ , the AGS transition operators (1) have simple poles, i.e., the energy-dependence of  $\mathcal{U}_{\beta\alpha}$  at  $E \approx -B_r$  can be given by

$$\mathcal{U}_{\beta\alpha} = \sum_{j=-1}^{\infty} \hat{\mathcal{U}}_{\beta\alpha}^{(r,j)} (E - E_r)^j. \quad (6)$$

The unstable bound state (UBS) pole in the complex energy plane is located in one of the unphysical sheets that is adjacent to the physical sheet [21]. The UBS therefore affects the physical observables leading to resonant effects in the four-boson collisions. As a consequence, the properties of those unstable tetramers can be extracted from the behavior of the four-boson scattering amplitudes or observables in the region  $|E + B_r| < \Gamma_r$  where the series (6) is approximated very well by few terms with  $j \leq 0$  or 1.

We solve the AGS equations (1) in the momentum-space partial-wave framework with two different types of basis states as explained in Refs. [12,20]. In this representation the AGS equations for each total angular momentum  $\mathcal{J}$  become a system of coupled integral equations in three continuous variables, the magnitudes of the Jacobi momenta  $k_x$ ,  $k_y$ , and  $k_z$  for the relative motion in the 1+1, 2+1, and 3+1 (1+1, 1+1, and 2+2) subsystems of the 3+1 (2+2) configurations, respectively. Although such equations can be solved as done in Refs. [15,16] for the four-nucleon scattering, the technical implementation is highly demanding. On the other hand, in this work we are interested in the universal properties of the four-boson system that must be independent of the short-range interaction details and therefore we can choose the most convenient form of the potential. The practical solution simplifies considerably by using a separable two-boson potential  $v = |g\rangle\lambda\langle g|$ . In this case the AGS equations (1) can be reduced to a system of integral equations with only two variables,  $k_y$  and  $k_z$ ; the details are given in Ref. [12].

The four-boson reactions from which we extract the tetramer properties involve at most one dimer-dimer channel but several (up to five in the present calculations) atom-trimer channels with the binding energies differing by many orders of magnitude. As pointed out in Ref. [12], this leads to additional difficulties that are very hard to overcome in the coordinate-space approaches but can be resolved reliably in our momentum-space framework: we discretize the integrals using Gaussian quadrature rules and use momentum grids of correspondingly broad range; each subsystem bound state pole of  $U_\alpha$  is isolated in a different subinterval when performing the integration over  $k_z$  [20]. The discretization of integrals in the AGS equations leads to a system of linear algebraic equations whose solution is described in Refs. [12,20].

### 3 Results

The interaction model is taken over from Ref. [8], i.e., we use a rank-1 separable potential limited to the  $l_x = 0$  state with the form factor

$$\langle k_x | g \rangle = [1 + c_2 (k_x/\Lambda)^2] e^{-(k_x/\Lambda)^2} \quad (7)$$

and the strength  $\lambda$  constrained to reproduce the given value of the scattering length  $a$  for two particles of mass  $m$ . The rank-1 potential supports at most one two-boson bound state, i.e., there are no deeply bound dimers.

The results will be presented as dimensionless ratios that are independent of the used  $\Lambda$  and  $m$  values in the universal limit. To demonstrate that our results are indeed independent of the details of the short-range interaction, we use two very different form factors with  $c_2 = 0$  and  $c_2 = -9.17$ .

#### 3.1 Unitary limit

We start by presenting the results in the unitary limit  $a = \infty$  where the dimer binding energy  $b_d$  vanishes but an infinite number of the trimers exists with a geometric spectrum of binding energies  $b_n = |\varepsilon_1^n|$ , i.e.,  $b_{n-1}/b_n \approx 515.035$ . This number was predicted analytically by Efimov [1] but our numerical calculations reproduce it very well for highly excited trimers, i.e., for  $n$  large enough such that the finite-range corrections become negligible. With  $n \geq 4$  we achieve at least six digit accuracy as demonstrated in Ref. [8] for both choices of the form factor (7). In contrast, significant deviations were found for the ground states, e.g.,  $b_0/b_1 \approx 548$  and 2126 with  $c_2 = 0$  and  $-9.17$ , respectively; this is caused by a very different short-range behavior of the two used models.

In our nomenclature we characterize the tetramers by two integers  $(n, k)$  where  $n$  refers to the associated trimer and  $k = 1$  (2) for a deeper (shallower) tetramer. Our preliminary predictions for the tetramer positions  $B_{n,k}$  and widths  $\Gamma_{n,k}$ , i.e., their relation to the associated trimer binding energy  $b_n$ , were given already in Ref. [8]. Here the study of tetramer properties is improved and extended. First we investigate the convergence of the results with respect to the number of included partial waves determined by the parameter  $l_{\max}$  such that  $l_y, l_z \leq l_{\max}$ . Example results for  $n = 4$  and  $c_2 = 0$  are collected in Table 1. The convergence is quite fast

$l_{\max}$	$B_{4,1}/b_4$	$\Gamma_{4,1}/2b_4$	$B_{4,2}/b_4$	$\Gamma_{4,2}/2b_4$
0	4.6754	0.01422	1.00404	$2.93 \times 10^{-4}$
1	4.6056	0.01474	1.00215	$2.30 \times 10^{-4}$
2	4.6108	0.01485	1.00228	$2.38 \times 10^{-4}$
3	4.6102	0.01484	1.00227	$2.38 \times 10^{-4}$

**Table 1** Convergence of  $n = 4$  tetramer properties with  $l_{\max}$  at  $a \rightarrow \infty$ . Form factor with  $c_2 = 0$  is used.

$n$	$B_{n,1}/b_n$	$\Gamma_{n,1}/2b_n$	$B_{n,2}/b_n$	$\Gamma_{n,2}/2b_n$
0	5.6402		1.04185	
1	4.5169	0.03363	1.00105	$3.82 \times 10^{-4}$
2	4.6035	0.01366	1.00216	$2.14 \times 10^{-4}$
3	4.6098	0.01471	1.00226	$2.36 \times 10^{-4}$
4	4.6102	0.01484	1.00227	$2.38 \times 10^{-4}$
5	4.6102	0.01483	1.00227	$2.38 \times 10^{-4}$
0	3.2192			
1	4.9923	0.01360	1.00996	$4.18 \times 10^{-4}$
2	4.6108	0.02084	1.00227	$3.34 \times 10^{-4}$
3	4.6098	0.01493	1.00226	$2.39 \times 10^{-4}$
4	4.6102	0.01483	1.00227	$2.38 \times 10^{-4}$
5	4.6102	0.01483	1.00227	$2.38 \times 10^{-4}$

**Table 2** Tetramer positions and widths in the unitary limit. Results obtained with  $c_2 = 0$  ( $c_2 = -9.17$ ) in Eq. (7) are given in the top (bottom) part.

but the nonzero angular momentum states for the 2+1 and 3+1 subsystems cannot be neglected. Our previous results of Ref. [8] obtained with  $l_{\max} = 2$  are already well converged, the inclusion of  $l_y = l_z = 3$  states yields only tiny corrections. Furthermore, we note that the contributions of even  $l_y, l_z$  are attractive while those of odd are repulsive.

In Table 2 we present our results for the positions  $B_{n,k}$  and widths  $\Gamma_{n,k}$  of the tetramer pairs up to  $n = 5$ ; they were obtained with  $l_{\max} = 3$ . The ratios  $B_{n,k}/b_n$  and  $\Gamma_{n,k}/2b_n$  for both choices of the potential form factor converge towards universal values

$$B_{n,1}/b_n = 4.610(1), \quad (8a)$$

$$\Gamma_{n,1}/2b_n = 0.01483(1), \quad (8b)$$

$$B_{n,2}/b_n = 1.00227(1), \quad (8c)$$

$$\Gamma_{n,2}/2b_n = 2.38(1) \times 10^{-4} \quad (8d)$$

as  $n$  increases. However, significant potential-dependent deviations due to finite-range effects can be seen for  $B_{n,k}/b_n$  and  $\Gamma_{n,k}/2b_n$  at  $n \leq 1$  and  $n \leq 2$ , respectively. With  $c_2 = -9.17$ , where the  $n = 0$  trimer is a non-Efimov-like state [8], the  $(0, 2)$  tetramer is even absent. Including a strong repulsive three-body force would decrease the binding energies and increase the size of the states and thereby speedup the  $n$ -convergence [4] but the ground state calculations ( $n = 0$ ) would be insufficient anyway since  $n = 0$  doesn't account for the inelastic collisions and finite width. This also explains why the convergence for  $\Gamma_{n,k}$  is slower than for  $B_{n,k}$ .

Next we study the effect of unstable tetramers on the elastic and inelastic cross sections  $\sigma(n \rightarrow n')$  in atom-trimer collisions;  $n$  and  $n'$  characterize the trimer state in the initial and final channel, respectively. To form dimensionless ratios for each

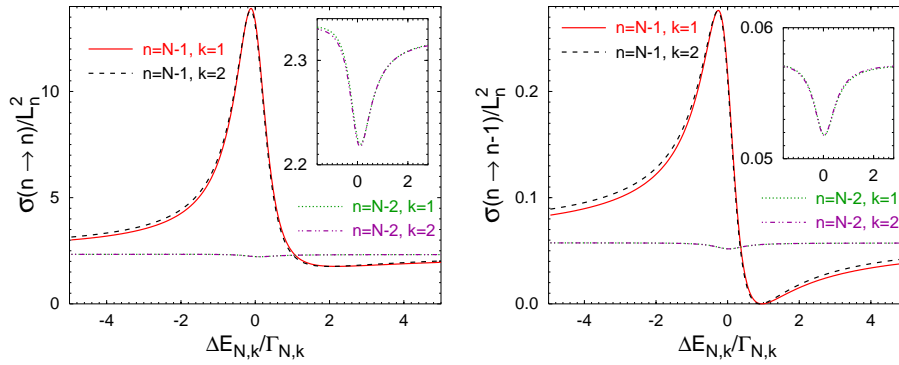


**Fig. 1** (Color online) Elastic and inelastic cross sections for the atom scattering from the  $n$ th trimer in the vicinity of the  $(N, k)$ th tetramer.

trimer we introduce the length scale  $L_n = \hbar/\sqrt{2\mu_1 b_n}$ . As already found in Ref. [8], for sufficiently large  $n$  and  $n'$  the ratios  $\sigma(n \rightarrow n')/L_n^2$  depend only on  $n - n'$  but not on the employed potential. Furthermore, for the inelastic cross sections ( $n' < n$ ) an additional relation  $\sigma(n \rightarrow n')/\sigma(n \rightarrow n' - 1) \approx 43.7$  was established [8]. Thus, in the universal limit the atom scattering from the  $n$ th trimer can be fully characterized by only two cross sections, the elastic one  $\sigma(n \rightarrow n)$  and the leading inelastic one  $\sigma(n \rightarrow n - 1)$ . In the case of  $\sigma(n \rightarrow n)$  the atom-trimer  $P$ - and  $D$ -wave contributions calculated in Ref. [8] have to be added; they are negligible for  $\sigma(n \rightarrow n - 1)$ . In Fig. 1 we study the behavior of the elastic and inelastic atom-trimer cross sections in the vicinity of the  $(N, k)$ th tetramer; we use  $c_2 = 0$  and  $N = 5$  such that the finite-range effects are negligible. We use the energy variable  $\Delta E_{N,k} = E + B_{N,k}$  that measures the distance to the tetramer position. Despite very different tetramer widths, the behavior of the cross section as function of  $\Delta E_{N,k}/\Gamma_{N,k}$  is very similar for  $k = 1$  and  $2$ . Although  $\mathcal{U}_{11}$  has pole in all open channels  $n < N$ , the elastic and inelastic cross sections  $\sigma(n \rightarrow n)$  and  $\sigma(n \rightarrow n - 1)$  have characteristic resonance peaks only in the case of  $n = N - 1$  where they increase by a factor of 5. For  $n \leq N - 2$  a minimum is seen close to  $\Delta E_{N,k} = 0$  which becomes less and less pronounced as the difference  $N - n$  increases; we therefore show only  $n = N - 2$  results where in the minimum the elastic (inelastic) cross section is decreased by 5% (10%). In accordance with this behavior the phase shift (not shown here) increases by  $180^\circ$  only for  $n = N - 1$  while local minima take place for  $n \leq N - 2$ .

### 3.2 Tetramers between four-atom and dimer-dimer thresholds

Trimers and the associated tetramers exist in a certain regime of large finite  $|a|$ . In Fig. 2 we show the tetramer positions  $B_{n,k}$  as functions of  $a$ ; we include also the binding energies in the atom-trimer and dimer-dimer channels,  $b_n$  and  $2b_d$ . As a reference point for  $a$  we choose the intersection of the dimer-dimer and the  $n$ th atom-trimer thresholds, i.e.,  $b_n = 2b_d$  at  $a = a_n^{dd}$ . All the binding energies are normalized by the  $n$ th trimer binding energy in the unitary limit  $b_n^u$ . In Fig. 2 we show  $B_{n,2}$  only at  $a < 0$ ; at  $a > 0$  the shallow tetramer lies very close the

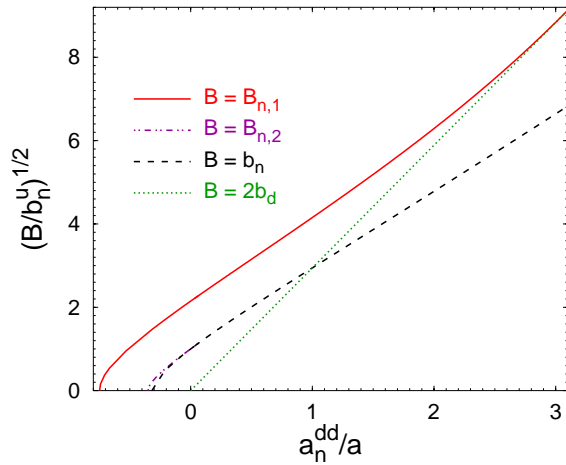


**Fig. 2** (Color online) Tetramer, trimer and dimer binding energies as functions of the two-boson scattering length.

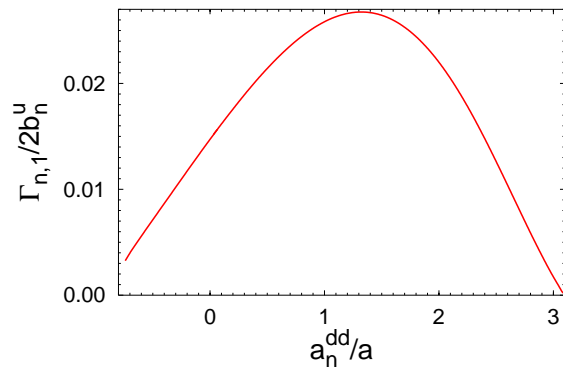


**Fig. 3** (Color online) The width of the deeper tetramer as a function of the two-boson scattering length.

atom-trimer threshold and exhibits a nontrivial behavior that will be presented separately in the next subsection. The  $a$ -evolution of the width  $\Gamma_{n,1}$  of the deeper tetramer is shown in Fig. 3.

As can be seen in Fig. 2, on the side of negative  $a$  the trimers (tetramers) emerge at the three (four) free atom threshold with zero energy. We denote by  $a_n^0$  and  $a_{n,k}^0$  the specific negative values of  $a$  where  $b_n = 0$  and  $B_{n,k} = 0$ , respectively. In an ultracold atomic gases these  $a$  values would correspond to a resonant enhancement of the three or four-atom recombination process [4, 6]. On the side of positive  $a$  the trimers decay via the atom-dimer threshold, i.e.,  $b_n = b_d$  at  $a = a_n^d$ ; this situation is outside the range of Fig. 2 since  $a_n^{dd}/a_n^d = 6.789(1)$  [9]. The tetramers decay via the dimer-dimer threshold, i.e.,  $B_{n,k} \approx 2b_d$  and  $\Gamma_{n,k} = 0$  at  $a = a_{n,k}^{dd}$ , leading to a resonant behavior of the dimer-dimer scattering length  $A_{dd}$  shown for  $k = 1$  in Fig. 4. The consequence of this phenomenon in an ultracold gas of dimers is a resonant enhancement of the trimer creation and dimer-dimer relaxation processes [5, 17, 9], the zero-temperature rate being  $\beta_{dd}^0 = -(8\pi\hbar/m)\text{Im}A_{dd}$ .

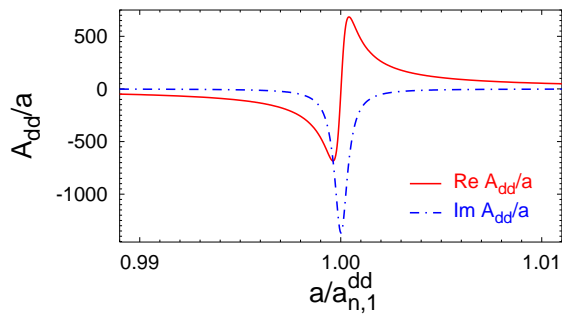


**Fig. 4** (Color online) Dimer-dimer scattering length as a function of the atom-atom scattering length in the vicinity of the  $k = 1$  tetramer intersection with the dimer-dimer threshold.

All those special values of  $a$  are related in a universal way provided  $n$  is sufficiently large. With the present interaction models the universal limit is reached with high accuracy at  $n = 4$  as can be seen in numerous examples for tetramer properties given in Table 2 and for various atom-trimer scattering observables in Ref. [8]. In particular, the convergence for the tetramer intersections with the dimer-dimer threshold is demonstrated in Ref. [9], yielding the ratios

$$a_{n,1}^{dd}/a_n^{dd} = 0.3235(1), \quad (9a)$$

$$a_{n,2}^{dd}/a_n^{dd} = 0.99947(2), \quad (9b)$$

where the uncertainties are estimated by comparing the predictions obtained with different  $n$  and  $c_2$ . For the intersection of the tetramers with the four free atom threshold we get

$$a_{n,1}^0/a_n^0 = 0.4254(2), \quad (10a)$$

$$a_{n,2}^0/a_n^0 = 0.9125(2). \quad (10b)$$

Furthermore, semi-analytical results [2] are available for some quantities of the three-boson nature, namely,  $a_n^d \sqrt{mb_n^u} = 0.0707645086901$  and  $-a_n^0 \sqrt{mb_n^u} = 1.56(5)$  for  $n \rightarrow \infty$ . They agree well with our numerical predictions

$$a_n^d \sqrt{mb_n^u} = 0.07076(1), \quad (11a)$$

$$-a_n^0 \sqrt{mb_n^u} = 1.5077(1) \quad (11b)$$

thereby confirming their reliability.

### 3.3 Shallow tetramer

Since the shallow tetramer lies very close to the associated atom-trimer threshold, we use a different representation to show the  $a$ -evolution of its position, namely, we consider its relative distance to the atom-trimer threshold  $(b_n - B_{n,2})/b_n^u$ . Together with the width it is presented in Fig. 5 in the whole region of its existence. For both tetramers the widths  $\Gamma_{n,k}$  remain finite at the respective  $a = a_{n,k}^0$  where  $B_{n,k}$  vanish; the  $k = 1$  case is shown in Fig. 3. The shallow tetramer detaches

most from the atom-trimer threshold around  $a \approx a_n^0$  where  $b_n$  almost vanishes. Most remarkably, at two special positive values of  $a = a_n^{v,j}$  the shallow tetramer intersects the atom-trimer threshold, i.e., when moving away from the unitary limit it first decays at  $a_n^{v,1}$ , then reappears at  $a_n^{v,2}$ , and finally decays via the dimer-dimer threshold at  $a = a_n^{dd}$ . In other words, the shallow tetramer in a particular regime  $a \in (a_n^{v,2}, a_n^{v,1})$  becomes an inelastic virtual state (IVS) [21] with  $\Gamma_{n,2} < 0$  instead of an UBS with positive width. The intersection points  $a_n^{v,j}$  correspond to  $\Gamma_{n,2} = 0$  and are universal, i.e.,

$$a_n^{v,1}/a_n^{dd} = 13.75(5) \quad (12a)$$

$$a_n^{v,2}/a_n^{dd} = 1.0016(1). \quad (12b)$$

In the vicinity of  $a = a_n^{v,j}$  the tetramer position  $B_{n,2} < b_n$  while otherwise  $B_{n,2} > b_n$ . Thus, it may seem that the tetramer IVS is mostly below the atom-trimer threshold. However, one has to keep in mind the changed sign of  $\Gamma_{n,2}$  for IVS that implies the change of the energy sheet. The IVS corresponds to the pole of the transition operators  $\mathcal{U}_{\beta\alpha}$  in the complex energy plane on one of the nonphysical sheets that is, in contrast to the one of UBS, more distant from the physical sheet [21]. For this reason the IVS affects the physical scattering observables in a completely different way as compared to UBS: the elastic and inelastic cross sections around  $E \approx -B_{n,2}$  for IVS, i.e., for  $a \in (a_n^{v,2}, a_n^{v,1})$  show no resonant peaks that were seen in Fig. 1 for the UBS. Thus, the parameters of the IVS cannot be extracted using Eq. (6). However, an approximate procedure based on the atom-trimer scattering length and effective range parameter as described in Ref. [22] was applied to obtain the IVS results in Fig. 5. The IVS pole only affects the physical observables when it is located extremely close to the atom-trimer threshold. In that case the cross sections and phase shift have a cusp exactly at the atom-trimer threshold, i.e., at  $E = -b_n$ , but the cusp disappears rapidly with increasing  $(B_{n,2} - b_n)$  and  $-\Gamma_{n,2}$ ; an examples can be found in Ref. [22]. We note that the tetramers become IVS also after crossing the dimer-dimer threshold, i.e., at  $a < a_n^{dd}$ .

The most prominent effect of the tetramer UBS-IVS conversions through the atom-trimer (dimer-dimer) threshold is a resonant enhancement of the atom-trimer scattering length  $A_n$  around  $a = a_n^{v,j}$  (dimer-dimer scattering length  $A_{dd}$  around  $a = a_n^{dd}$ ); thus, at the corresponding  $a$  values  $A_n$  exhibits qualitatively the same behavior as shown for  $A_{dd}$  in Fig. 4. The regime around  $a_n^{v,j}$  is not yet explored experimentally. However, in an ultracold mixture of atoms and excited trimers tuning the atom-atom scattering length to the values close to  $a_n^{v,j}$  would lead to a resonantly increased rate of the atom-trimer relaxation whose zero-temperature limit is  $\beta_n^0 = -(4\pi\hbar/\mu_1)\text{Im}A_n$ . Of course, in real experiments the resonance positions may deviate from the universal values (12) due to finite-range effects.

### 3.4 Comparison with previous works

A number of numerical techniques is available for the four-boson bound state calculations, both in the momentum [3,10] and coordinate space [4,11]. Some of them [4], neglecting the finite width of the higher tetramers, were used to find

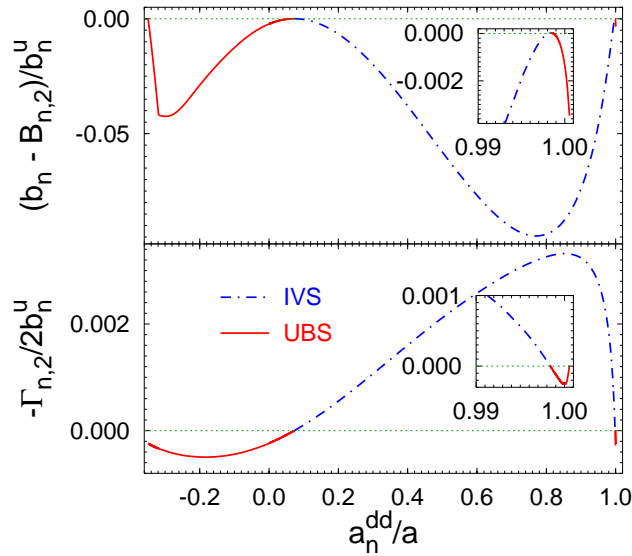


**Fig. 5** Position of the shallow tetramer relative to the atom-trimer threshold (top) and its width (bottom) as functions of the two-boson scattering length  $a$ . We used  $b_n = 0$  at  $a_n^{dd}/a < a_n^{dd}/a_n^0 \approx -0.3186$  where the  $n$ th trimer doesn't exist.

their energies and threshold intersection points. The results of Refs. [4,17] for  $B_{n,k}/b_n$  at unitarity,  $a_{n,k}^0/a_n^0$ , and  $a_{n,k}^{dd}/a_n^{dd}$  agree with ours within few percents. Those calculations [4,17] were limited to  $n \leq 1$  or 2 where the finite-range effects could not be entirely neglected and the convergence with  $n$  was not better than few percents; this is consistent with our findings as can be seen in Table 2, albeit with different potentials. We demonstrated that higher  $n$  are needed to achieve the universal limit accurately; this is technically very demanding, especially in the coordinate-space framework.

However, in contrast to our work, Ref. [4] has not predicted the shallow tetramer intersections with the atom-trimer threshold at  $a_n^{v,j}$ . It appears that the results of Refs. [4,17] are quite poorly converged for the fine-scale quantities  $(B_{n,2}/b_n - 1)$  at unitarity and  $(1 - a_{n,2}^{dd}/a_n^{dd})$ . For the former our five best-converged results are 0.00227 within 0.5% according to Table 2 while the three best-converged results of Ref. [4] are 0.006, 0.03, and 0.001. For  $(1 - a_{n,2}^{dd}/a_n^{dd})$  the prediction of Ref. [17], 0.019, overestimates our well-converged result 0.00053 by a factor of 35. Both these deviations indicate that Refs. [4,17] strongly overestimate the distance of the shallow tetramer from the atom-trimer threshold such that they never cross each other. We note that the nonuniversal (0,2) tetramer of our work is also bound considerably stronger than the universal ones and therefore doesn't intersect the atom-trimer threshold.

#### 4 Summary

We studied universal bosonic tetramers that are unstable bound states in the continuum and strongly affect collisions in the four-boson system. We extracted the

tetramer properties such as positions, widths, and limits of existence from the behavior of the atom-trimer and dimer-dimer scattering observables. These collision processes were described using exact four-particle scattering equations for the transition operators that were solved in the momentum-space framework with high precision. A rigorous treatment of the four-boson continuum enabled us to determine the widths of the tetramers that were out of reach in previous works. Furthermore, we accurately achieved the universal limit by considering reactions involving high excited trimers where the finite-range effects are negligible. In this respect our results are much better converged than those of previous works [4, 17] where only the tetramer positions and existence limits have been calculated. While the agreement between our predictions and those of Refs. [4, 17] is reasonable for the more tightly bound tetramer, there are drastic differences for the shallow one. We demonstrate that changing the two-boson scattering length the shallow tetramer intersects the atom-trimer threshold twice and in a special regime becomes an inelastic virtual state; these UBS-IVS conversions lead to resonant effects in ultracold atom-trimer collisions.

## References

1. Efimov, V.: Energy levels arising from resonant two-body forces in a three-body system. *Phys. Lett. B* **33**, 563 (1970).
2. Braaten, E., Hammer, H.-W.: Universality in few-body systems with large scattering length. *Phys. Rep.* **428**, 259 (2006).
3. Hammer, H. W., Platter, L.: Universal properties of the four-body system with large scattering length. *Eur. Phys. J. A* **32**, 113 (2007).
4. von Stecher, J., D’Incao, J. P., Greene, C. H.: Signatures of universal four-body phenomena and their relation to the Efimov effect. *Nature Phys.* **5**, 417 (2009).
5. Ferlaino, F., Knoop, S., Mark, M., Berninger, M., Schöbel, H., Nägerl, H.-C., Grimm, R.: Collisions between Tunable Halo Dimers: Exploring an Elementary Four-Body Process with Identical Bosons. *Phys. Rev. Lett.* **101**, 023201 (2008).
6. Ferlaino, F., Knoop, S., Berninger, M., Harm, W., D’Incao, J. P., Nägerl, H.-C., Grimm, R.: Evidence for Universal Four-Body States Tied to an Efimov Trimer. *Phys. Rev. Lett.* **102**, 140401 (2009).
7. Pollack, S. E., Dries, D., Hulet, R. G.: Universality in Three- and Four-Body Bound States of Ultracold Atoms. *Science* **326**, 1683 (2009).
8. Deltuva, A.: Efimov physics in bosonic atom-trimer scattering. *Phys. Rev. A* **82**, 040701(R) (2010).
9. Deltuva, A.: Universality in bosonic dimer-dimer scattering. *Phys. Rev. A* **84**, 022703 (2011).
10. Yamashita, M. T., Tomio, L., Delfino, A., Frederico, T.: *Europhys. Lett.* **75**, 555 (2006).
11. Blume, D., Greene, C. H.: Monte Carlo hyperspherical description of helium cluster excited states. *J. Chem. Phys.* **112**, 8053 (2000).
12. Deltuva, A., Lazauskas, R., Platter, L.: Universality in few-body scattering. *Few-Body Syst.* **51**, 235 (2011).
13. Lazauskas, R., Carbonell, J.: Description of He<sub>4</sub> tetramer bound and scattering states. *Phys. Rev. A* **73**, 062717 (2006).
14. Grassberger, P., Sandhas, W.: Systematical treatment of the non-relativistic n-particle scattering problem. *Nucl. Phys.* **B2**, 181 (1967); E. O. Alt, P. Grassberger, and W. Sandhas, JINR report No. E4-6688 (1972).
15. Deltuva, A., Fonseca, A. C.: Four-body calculation of proton-<sup>3</sup>He scattering. *Phys. Rev. Lett.* **98**, 162502 (2007).
16. Deltuva, A., Fonseca, A. C., Sauer, P. U.: Four-nucleon system with  $\Delta$ -isobar excitation. *Phys. Lett. B* **660**, 471 (2008).
17. D’Incao, J. P., von Stecher, J., Greene, C. H.: Universal Four-Boson States in Ultracold Molecular Gases: Resonant Effects in Dimer-Dimer Collisions. *Phys. Rev. Lett.* **103**, 033004 (2009).

- 
18. Yakubovsky, O. A.: On the integral equations in the theory of N particle scattering. *Yad. Fiz.* **5**, 1312 (1967) [*Sov. J. Nucl. Phys.* **5**, 937 (1967)].
  19. Deltuva, A., Fonseca, A. C.: Ab initio four-body calculation of  $n$ - $^3\text{He}$ ,  $p$ - $^3\text{H}$ , and  $d$ - $d$  scattering. *Phys. Rev. C* **76**, 021001(R) (2007).
  20. Deltuva, A., Fonseca, A. C.: Four-nucleon scattering: Ab initio calculations in momentum space. *Phys. Rev. C* **75**, 014005 (2007).
  21. Badalyan, A. M., Kok, L. P., Polikarpov, M. I., Simonov, Y. A.: Resonances in coupled channels in nuclear and particle physics. *Phys. Rep.* **82**, 31 (1982).
  22. Deltuva, A.: Shallow Efimov tetramer as inelastic virtual state and resonant enhancement of the atom-trimer relaxation. *EPL* **95**, 43002 (2011).